Available online at www.sciencedirect.com

SciVerse ScienceDirect

Journal of the European Ceramic Society 32 (2012) 2723–2729

www.elsevier.com/locate/jeurceramsoc

Soda-lime glass-coating containing silver nanoparticles on Ti–6Al–4V alloy

L. Esteban-Tejeda [a], B. Cabal [a,*], F. Malpartida [b], R. López-Piriz [c], R. Torrecillas [c], E. Saiz [d], A.P. Tomsia [e], J.S. Moya [a]

[a] *Department of Biomaterials and Bioinspired Materials, Materials Science Institute of Madrid (ICMM-CSIC), Cantoblanco, Madrid 28049, Spain*
[b] *Department of Microbial Biotechnology, National Center for Biotechnology (CNB-CSIC), Cantoblanco, Madrid 28049, Spain*
[c] *Nanomaterials and Nanotechnology Research Center (CINN-CSIC-UO-PA), Parque Tecnológico de Asturias, Llanera 33428, Spain*
[d] *Centre for Advanced Structural Ceramics, Department of Materials, Imperial College London, Exhibition Road, London, UK*
[e] *Materials Sciences Division, Lawrence Berkeley National Laboratory, Berkeley, CA 94720, USA*

Available online 18 March 2012

Abstract

The prevention and treatment of post-surgical infections is an ongoing concern. Post-surgical infections often cannot be treated with commercially available antibiotic-loaded bone cement as because higher doses of antibiotics are required. We describe here an approach to prevent implant infection through the use of glass coatings combined with silver nanoparticles deposited by sedimentation and heat-treated at 980 °C on titanium alloys. Silver is nontoxic to the human tissue and has been used as an anti-infective for centuries. The glass/silver coatings are composed of a soda-lime glassy matrix containing silver nanoparticles ranging from 2.6 to 20 wt.%. Optimum firing conditions have been determined for the fabrication of coatings that adhere well to the metal implant. These final coatings do not crack or delaminate. The biocidal activity of these coatings was also investigated. Coatings containing 20 wt.% of silver nanoparticles exhibited excellent biocidal activity ($\log \eta > 5$) against Gram+, Gram− bacteria, and yeast after 24 h.

Keywords: Titanium alloy; Silver nanoparticles; Glass; Biocide; Medical implants

1. Introduction

Medical implants are becoming more common in industrialized societies as their population sage and life expectancies increase. Around 25 million of Americans have at least one medical implant.[1] In 2003, more than 700,000 dental implant procedures were performed in the United States; more than 1.3 million were performed in Europe.[2] In 2006, it was reported that approximately 1 million artificial hips and knees were being implanted each year in the United States.[3] Hip and knee replacements have a success rate of more than 90%, and dental implants fare better, at 90–95%.[4] However, metallic implants are prone to infections following surgery and are significant cause of morbidity[5,6]; and billions of dollars are spent annually to treat infectious diseases. Infections of the implants, very often in the form of biofilm, are the most common of complications and occur in 1–4% of cases.[7] A biofilm is an accumulation of microorganisms (bacteria, fungi, etc.) and cannot be easily eliminated from an implant. Despite the availability of excellent (albeit toxic) antibiotics such as imipenem and tobramycin, a joint replacement infection will often require removal of the implanted joint.[8,9] Antibiotic-loaded cement is frequently used when revision surgery is necessary. However some clinicians have raised concerns about its cost, the risk of developing antibiotic resistant strains of bacteria, and the potential for long-term mechanical failure.[10–15] While the percentage of failure for dental implants is very low – approximately 5% – it is typically the result of infection, accelerated bone loss, or poor osseointegration with loosening of the implant.[4] Therefore, prevention of biofilm formation around dental implants is important, as it may cause periimplantitis, an infection that constitutes the most important risk for bone loss and affect the long time survival of the implants.[4]

Because of their high strength, hardness, and superior fracture and fatigue resistance, metallic materials such as Ti-based alloys, CoCr-based alloys, or stainless steel are presently regarded as

* Corresponding author.
E-mail address: b.cabal@cinn.es (B. Cabal).

0955-2219/$ – see front matter © 2012 Elsevier Ltd. All rights reserved.
doi:10.1016/j.jeurceramsoc.2012.02.053

the materials-of-choice for load-bearing implant applications. However, strong metallic implants have well-documented fixation problems and cannot self-repair or adapt like natural bone to changing physiological conditions. Metals have been shown to generate adverse host responses as a result of wear or electrochemical corrosion. Particle debris can provoke local inflammatory and osteolytic responses, while electrochemical corrosion may produce degradation products (e.g., metal ions) that may result in clinical failure of the implant or an undesirable systemic host response. The growing incidence of infections occurring after total knee or total hip replacement surgery requires novel and effective antimicrobials. The need for these is particularly great for prophylactic applications.

Silver has been used to treat infections for centuries and is considered nontoxic to human tissue. Silver ions are capable of killing a wide range of Gram negative and positive bacteria and strains commonly found following arthoplasty, including methicillin-resistant *Staphylococcus aureus* (MRSA) and other antibiotic-resistant bacteria. Surprisingly, the sequence of events and the mechanism(s) involved in killing bacteria with silver ions while sparing human cells are not well-understood. There is little scientific literature describing the use of silver coatings on implant surfaces to improve antimicrobial action, and most of it concerns the use of silver-loaded antibacterial bone cement.[16–19] New strategies to prevent infections are clearly needed. For example, it is possible to raise the antimicrobial activity of the current metallic dental implants through surface modifications either by applying novel ceramic coatings or by patterning the implant's surfaces with silver nanoparticles.[20]

The present work explores the feasibility of using glass, combined with uniformly distributed silver nanoparticles, as novel antimicrobial coatings on Ti implants. The glass/silver coatings are composed of a soda-lime glassy matrix containing silver nanoparticles in three concentrations: 2.6, 10, and 20 wt.%. The experiments were designed to evaluate the antimicrobial activity of these coatings, to determine their mechanical properties (adhesion to Ti6Al4V), and to optimize the glass/Ag compositions.

Our findings provide valuable insight into the biocidal behavior of the coatings, and pave the way for future work aimed at optimizing the biological and mechanical performance of such structures.

2. Materials and methods

2.1. Materials

The starting materials were (i) a commercial soda-lime glass from the SiO_2–Na_2O–K_2O–CaO–MgO–B_2O_3 system with the following chemical composition (wt.%): 70.2 SiO_2, 15.8 Na_2O, 7.1 CaO, 3.2 MgO 1.06, B_2O_3, 0.05 K_2O, 1.71 Al_2O_3, 0.02 Fe_2O_3, and 0.86 others with a deformation point ~668 °C and (ii) vitellinate/nAg (Batch n° 127, ARGENOL S.L.), which is a protein of high molecular weight with a particle size distribution of $d_{50} \approx 10 \pm 2$ nm. This sample was fully characterized in a previous work[21] by differential thermal analysis (DTA), thermogravimetry (TG), X-ray diffraction (XRD), ultraviolet–visible absorption spectroscopy (UV–vis spectroscopy), and transmission electron microscopy (TEM). The chemical analysis was determined by inductively coupled plasma (ICP) and was found to be 20 wt.% of silver and 7.6 wt.% of sodium oxide.

In order to evaluate the role of silver in the wettability of the silver doped glass, silver free glasses with sodium oxide concentrations equal to the corresponding glassy matrices of the silver doped glasses were prepared as follows: (i) the glasses were prepared using reagent grade SiO_2 (Cuarzos Industriales S.A., Santiago de Compostela), α-Al_2O_3 (Taimei Chemical Co. Ltd., Japan), H_3BO_3, Na_2CO_3, and $CaCO_3$ (Sigma–Aldrich); (ii) the starting materials were mixed thoroughly and heated in platinum crucibles at 850 °C for 1 h to favour decarbonation of samples; and (iii) subsequently, they were melted at 1400 °C for 1 h, and then quenched into water. All the obtained glasses were found to be transparent.

2.2. Coating

Silver-doped glass powders with varying silver concentrations (2.6, 10, and 20 wt.%) were obtained following a similar procedure as that described in the previous work.[21] The soda-lime glass (<32 μm) and the corresponding fraction of vitellinate/nAg were homogeneously blended in isopropyl alcohol overnight under constant stirring at 30 rpm. After the suspensions were dried at 60 °C for 4 h, the homogeneous mixtures were uniaxially pressed into pellets (Ø ~ 10 mm) at 250 MPa. Next, they were sintered in air in two steps; by heating at a rate of 3 °C/min to 500 °C and to 725 °C, respectively, and holding for 1 h. Tubular electrical furnace and zirconia crucibles were used. The obtained glass/nAg pellets were milled down to <32 μm in a planetary ball mill. These powders were fully characterized by XRD using a Bruker D8 diffractometer using CuKα radiation working at 40 kV and 30 mA in a step-scanning mode from 5° to 70° with a step width of 0.0288° and a step time of 2.5 s, by scanning electron microscopy (SEM) (Hitachi S-4300) and transmission electron microscopy (TEM) (JEOL FXII at 200 kV). Optical absorption spectrum was measured in a range from 200 nm to 800 nm, using a JASCO UV-Vis V-660 spectrophotometer to determine the surface plasmon resonance of silver nanoparticles.

Cladding of Ti–6Al–4V plates (99.0% purity and 12.5 mm × 8.3 mm × 1 mm) was performed by deposition of these powders (0.2 g), with a particle size distribution of $d_{50} = 11.56 \pm 0.03$ μm, from homogeneous suspension in acetone (20 mL) and subsequently air-dried at 40 °C. Afterwards, the coated plates were heated in an argon atmosphere at 980 °C for 1 h.

2.3. Characterization of the coating

The sessile drop method has been chosen to study the contact behavior between the titanium alloy substrate and the different coatings. Sessile drop experiments were performed on Ti–6Al–4V plates in an argon atmosphere at 980 °C for 1 h. For this purpose, pseudospheres (Ø ~ 10 mm) were made by cold isostatic pressed at 150 MPa, using the same silver-doped

glass powders employed for the coatings. Similar experiments were carried out with the silver free glasses to clarify the role of silver. Surface and cross-section morphology and composition of the coated samples were analyzed by scanning electron microscopy (SEM) coupled with energy dispersive spectroscopy (EDS) (Hitachi S-4300).

The interface Ti alloy/silver-doped glassy matrix was studied by transmission electron microscopy (TEM) using a JEOL FXII operating at 200 kV. Samples for TEM interface analysis were prepared by cutting cross-sections of the glass/alloy interface. The sections were ground to a thickness of 80 μm and fixed into a Cu mesh (3 mm of diameter). The disks were polished to less than 20 μm and milled by argon-ion milling.

XRD analyses of these samples were carried out in a Bruker D8 diffractometer using CuKα radiation working at 40 kV and 30 mA in a step-scanning mode from 10° to 70° with a step width of 0.028° and a step time of 2.5 s. Microindentation tests were performed using a Buehler Micromet 5103 Digital Microindentation Hardness Tester with Vickers indenter.

2.4. Biocidal activity test

The antimicrobial benefits of the coatings were evaluated against three different microorganisms: *Escherichia coli JM110* (Gram-negative bacteria), *Micrococcus luteus* (Gram-positive bacteria) and *Issatchenkia orientalis* (yeast). The microorganisms were incubated overnight at 37 °C in a suitable liquid media (i.e., Luria Bertani [LB] for *E. coli* and *M. luteus*, or yeast extract dextrose [YEPD] for *I. orientalis*). Before the experiments, 10 μL from each culture were diluted into 1 mL of a suitable media and cultured at 37 °C for 6 h. Subsequently, Ti alloy plates coated with different silver-doped glasses (2.6, 10, and 20 wt.% nAg) were added. The following controls were used: a silver-free media (culture containing the corresponding nutrient and the microorganisms without the Ti plates) and Ti alloy coated with silver-free glass (culture containing the corresponding nutrient, microorganisms and glass coated plate). The survivals rates from each culture were counted after 24 h by plating serial dilution. At the end of the growing period, cells were removed by centrifugation and the release of silver to the fermentation broth was determined by inductively coupled plasma (ICP) (ICP Perkin Elmer mod. optima 2100 DV).

3. Results

3.1. Coatings

The characterization by UV–vis analysis and TEM of the silver doped glasses powders are shown in Fig. 1A, C and D. A size distribution of globular-shaped silver nanoparticles, ranging

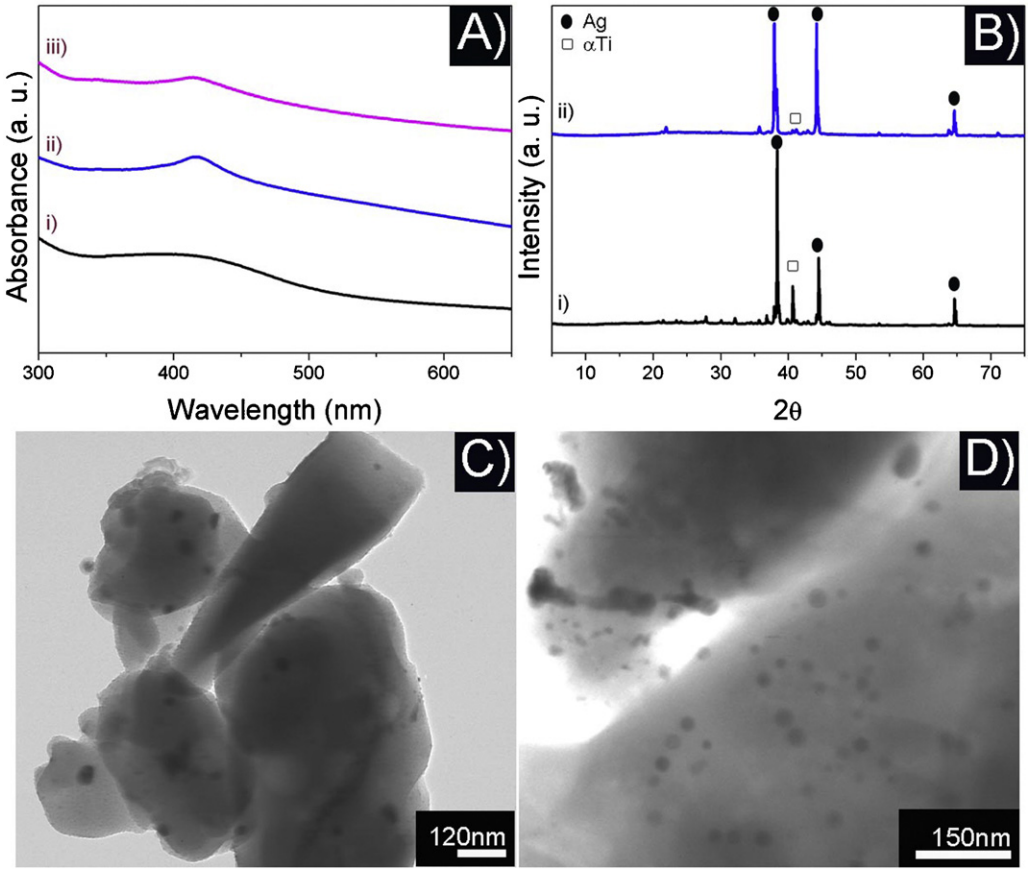

Fig. 1. (A) UV–vis spectra of (i) vitellinate/nAg and titanium alloy plates coated with different silver doped glasses: (ii) 2.6 wt.% nAg and (iii) 20 wt.% nAg. XRD patterns of titanium alloy coated with silver doped glasses: (i) 10 wt.% nAg and (ii) 20 wt.% nAg. (C and D) TEM micrographs of silver doped glass powders with different concentration of silver: 2.6 wt.% nAg and 20 wt.% nAg, respectively.

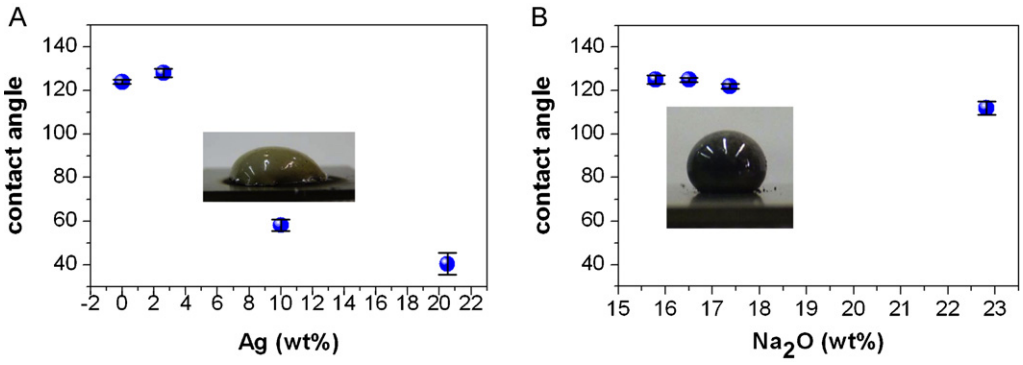

Fig. 2. Contact angle versus the content of (A) silver and (B) sodium oxide in the glassy matrix on titanium alloy substrates at 980 °C for 1 h in argon atmosphere. Insets correspond to glass-nAg (10 wt.% nAg) sessile drop (A), and silver free glass with a concentration of Na_2O (i.e., 17.5 wt.%) equal to the glassy matrix of the previous composition (B).

between 3 and 50 nm, homogeneously distributed in the glassy matrix, can be observed. XRD patterns of the titanium alloy coated with: (i) 10 wt.% nAg and (ii) 20 wt.% nAg are shown in Fig. 1B. In both cases, Bragg's reflections corresponding to metallic silver (i.e., $2\theta = 38.2°$, 44.4° and 64.6°, JCPDS 87-0720) are clearly visible. The rest of the peaks can be assigned to sodium calcium silicates due to partial devitrification on cooling of the glassy matrix. This effect is more significant in the sample with lower content of silver due to its higher fraction of glassy matrix. The phase α-Ti is also identified in all the samples.

Coatings were characterized by different techniques. The contact angles of silver-doped glasses (2.6, 10, and 20 wt.% nAg), as well as the corresponding glassy matrices on titanium alloy substrates, were studied by the sessile drop method. Results are shown in Fig. 2. Final concentration of sodium oxide in the glassy matrix depends on the final concentration of silver nanoparticles; the starting vitellinate/nAg contains 7.6 wt.% of sodium oxide. With higher concentration of silver nanoparticles, the content of sodium oxide in the glassy matrix will also increase.

To determine the fraction of β phase as well as the mechanical stability of the titanium alloy substrates, the Ti alloy plates were subjected to different thermal treatments at 980 °C, 1190 °C, and 1215 °C for 1 h in an argon atmosphere. After the thermal treatments, the fraction of β phase in each Ti alloy plate was determined by X-ray diffraction. Considering that the mass absorption coefficient (μ) in all the samples is the same and the angles of the selected peaks are very closed (2θ ranges from 37° to 40°), the fraction of β phase can be quantified using the equation described by Evans et al.[22]:

$$X_\beta = \frac{I_{\beta(1\,1\,0)}}{I_{\beta(1\,1\,0)} + I_{\alpha(0\,0\,2)} + I_{\alpha(1\,0\,1)}} \quad (1)$$

where $I_{\alpha(0\,0\,2)}$, $I_{\alpha(1\,0\,1)}$ and $I_{\beta(1\,1\,0)}$ are the area of the corresponding peaks. The fraction of β phase versus the temperature of the thermal treatment is plotted in Fig. 3. The micrographs corresponding to micro indentation prints after different heat treatments are also included in Fig. 3.

The mechanical stability of the Ti alloy plates at room temperature and heated at different temperatures was analyzed measuring Vickers hardness by micro indentation tests. The Vickers hardness values were found to be (kg/mm^2): 354.8 ± 7 for the plate at room temperature, 327.7 ± 8, 347.2 ± 10, and 675.0 ± 34 for the plates heated at 980 °C, 1190 °C, and 1215 °C, respectively.

SEM micrograph of the cross-section of 2.6 wt.% nAg sessile drop is shown in Fig. 4. Most of the silver nanoparticles are located bathe liquid–vapor interface, leading to the formation of some agglomerates.

The SEM micrographs of the top surface of the different coatings are shown in Fig. 5. Silver particles are homogeneously distributed. The sample with the highest silver content (i.e., 20 wt.% nAg) exhibits some spherical agglomerates ranging between 1 and 5 μm in diameter.

The interface between the titanium alloy substrate and the silver-doped glass was evaluated by SEM-EDS and TEM of the cross section. The thickness of all coatings was found to be ~25 μm. SEM micrograph and SEM-EDS line analysis of cross section of Ti alloy/silver doped glass coating (2.6 wt.% nAg) are displayed in Fig. 6A and B, respectively. TEM micrograph of

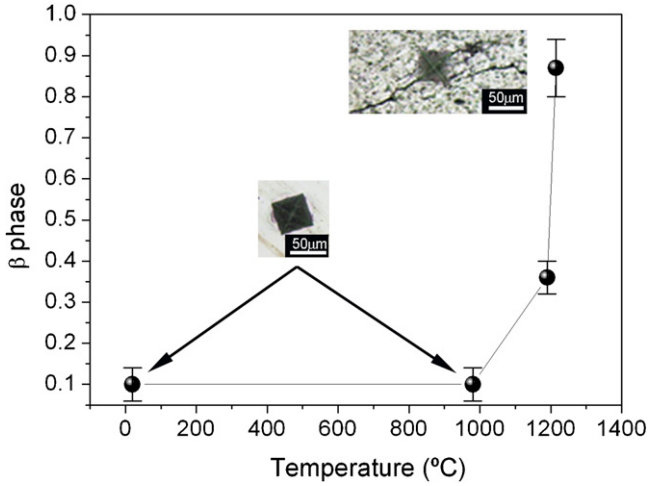

Fig. 3. Content of β phase for titanium alloy substrates, at room temperature and heated at different temperatures in argon atmosphere. Images of the indentation impressions on the Ti alloy plates at room temperature and heated at 980 °C and at 1215 °C, respectively, are inserted.

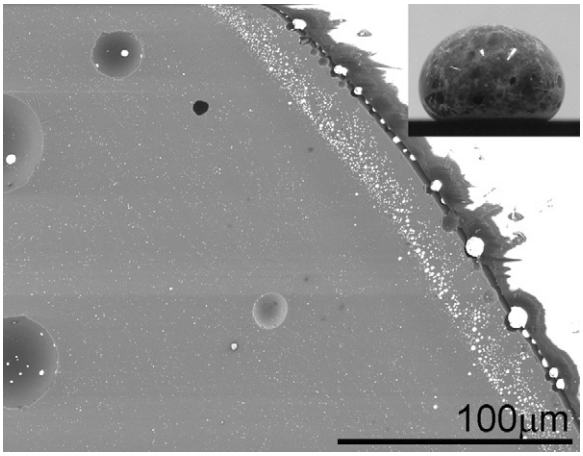

Fig. 4. SEM micrograph of the cross section of Ti alloy/glass (2.6 wt.% nAg) sessile drop after treatment at 980 °C for 1 h in argon atmosphere.

the cross section of Ti alloy/silver doped glass coating (20 wt.% nAg) is shown in Fig. 6C.

3.2. Biocide tests

The logarithm reduction ($\log \eta$) has been used to characterize the effectiveness of the biocide agent:

$$\log \eta = \log A - \log B \quad (2)$$

where A is the average number of viable cells from inoculum control after 24 h, and B is the average number of viable cells form substance after 24 h. For all the coatings studied only the sample with 20 wt.% silver nanoparticles was active against the three microorganisms tested, achieving a logarithm reduction higher than 5, meaning complete disinfection (Fig. 7).

4. Discussion

It is well known that silver nanoparticles display a surface plasmon around 400 nm. The precise position and the shape of the band depend on the environment of the nanoparticles and also on their size and shape.[23–25] As shown in Fig. 1A, absorption bands of silver-doped glass powders (2.6 and 20 wt.% nAg) are narrower in comparison with vitelinate/nAg, which could be attributed to the rupture of soft agglomerates present in the raw material (vitelinate/nAg). In the case of the sample with 20 wt.% nAg, the absorption band is wider than 2.6 wt.% nAg, due to the higher content of silver in the glassy matrix as well as the coarsening of silver nanoparticles.

To evaluate the suitability of these glasses to coat titanium, we performed the measurements of contact angle as a function of glass composition and silver content. Lower contact angles would favor the formation of thin, homogeneous and stable coatings. Increasing sodium content in the glasses has a negligible effect on wettability (Fig. 2B).[26] However, the silver nanoparticles have very strong effect and at the 10 wt.% Ag, the contact angle decreased in half, to 60° (Fig. 2A). This cannot be attributed to the observed Ag segregation to the solid–liquid interface, as this would decrease the corresponding interfacial energy and increase the obtuse contact angle of the liquid. This can only be attributable to the migration of the Ag to the Ti/glass interface, where it alloys with the metal (Fig. 6B).

All the coating fabrication was performed at 980 °C, where no degradation of the Ti alloy is expected. At the coating

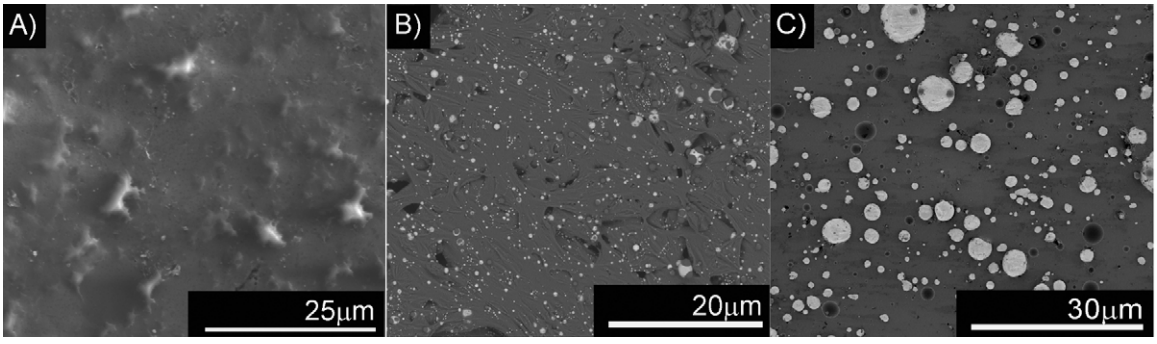

Fig. 5. SEM micrographs of titanium alloy plates coated with different silver doped glasses: (A) 2.6 wt.% nAg, (B) 10 wt.% nAg and (C) 20 wt.% nAg.

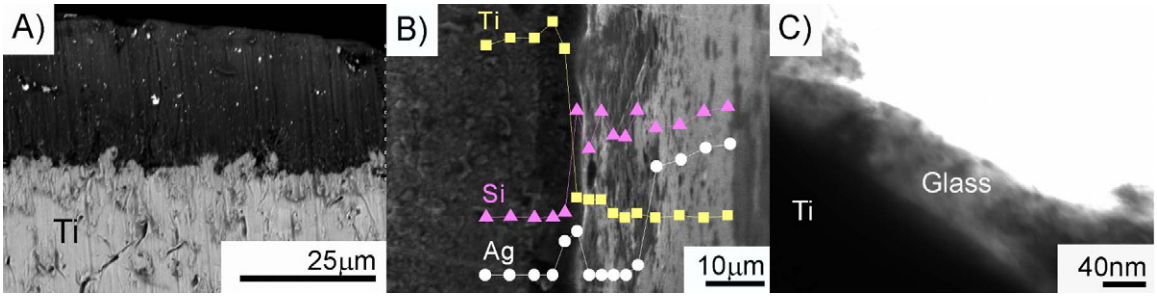

Fig. 6. (A) SEM micrograph of the cross section of Ti alloy/silver doped glass (2.6 wt.% nAg), (B) elemental line analysis (calibrated EDS) along the cross section of Ti alloy/silver doped glass (2.6 wt.% nAg) and (C) TEM micrograph of the cross section of Ti alloy/silver doped glass (20 wt.% nAg).

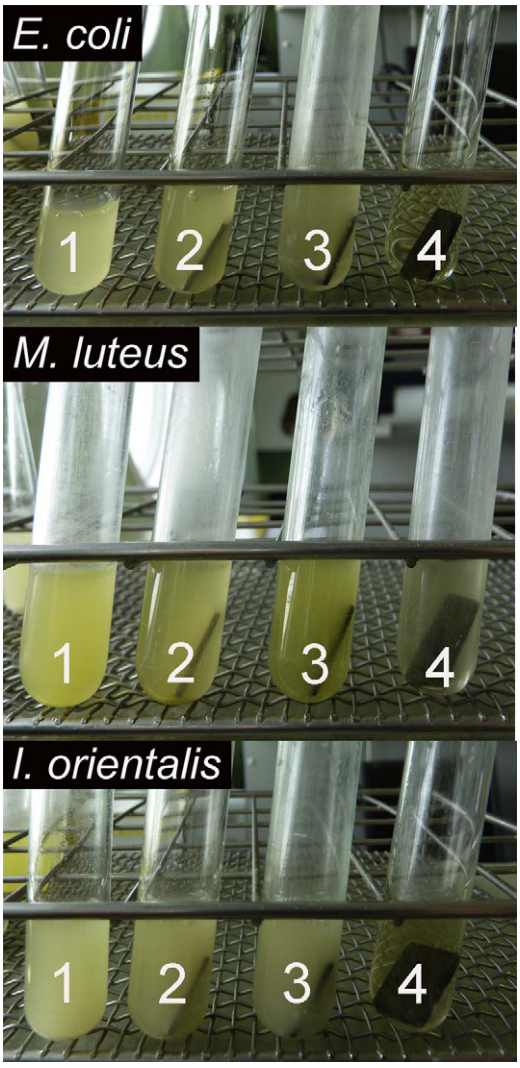

Fig. 7. Images after biocide test. The numbers stand for (1) control culture composed by nutrient and microorganisms, (2) culture with Ti alloy plate, (3) culture with Ti alloy plate coated by glass and (4) culture with Ti alloy plate coated by silver doped glass (20 wt.% nAg).

temperature of 980 °C, the Ag particles are molten and they coalesce to form micron-sized spheres. The contact angle of molten Ag on oxides is relatively high (>90°),[27] therefore during the densification of the coatings the melt is unstable in the porous space due to high contact angle and is exuded from the glass toward the solid–liquid and liquid–vapor interfaces.[28]

The molten silver that is exuded to the glass/Ti interface will alloy with the metal, while the glass also reacts with the substrate to form silicides. According to Ti–Ag and Ti–Si–Ag phase diagrams,[29,30] at 980 °C, β-Ti (ss), Ti_3Si, and TiAg are solid-state compatible compounds, which can be formed at the interface. The EDS analysis (Fig. 6B) confirms the presence of Si and Ag at the interface. The interfacial layer provides good interfacial adhesion[26]; and as a consequence, a good joining of the glass/Ti substrate was observed, as shown in the TEM micrograph of Fig. 6C.

The exudation of silver toward the surface of the coating favors its contact with the surrounding media, and a minimum amount of silver is needed to have a measurable biocidal effect. Only the plates coated with the highest concentration of silver nanoparticles (i.e., 20 wt.% nAg) were active against the three microorganisms tested, in the conditions in which the experiments were carried out. One of the main advantages that offers the incorporation of silver nanoparticles into a glassy matrix is that silver release rate is regulated in a controlled manner, providing long-term antibacterial characteristics. The release rate is directly dependent to the overall rate on glass degradation. In this way, an excessive release of the metal is avoided, otherwise it could be toxic. The concentrations of silver in the supernatant solutions after the biocide tests were ∼10 ppm for all the microorganisms studied. This value is lower than that of the toxic limit for osteoblasts (30 ppm),[31] which is important if the coatings are to be used on orthopedic implants. If the silver nanoparticles were exposed directly on the surface without anything that enabled a controlled release, the total released silver could not be in the acceptable cyto-/biocompatible range. Some examples of cytotoxicity can be found in the literature, e.g., Zhao et al.[32] introduced different concentrations of silver nanoparticles into titania nanotubes. They concluded that the samples showed some cytotoxicity and further works to control the silver release were required. Song et al.[33] showed that at high silver concentration (0.21–0.45 wt.%) the coatings exhibit cytotoxicity.

Further studies about the prevention of biofilm formation on the obtained glass-nAg coatings on Ti–6Al–4V alloys are in progress and will be the subject of a future publication.

5. Conclusion

On the basis of the results obtained in the present investigation, the following conclusions can be drawn:

1. A mechanically stable soda-lime coating (∼25 μm thickness) containing silver nanoparticles, ranging from 2.6–20 wt.%, on Ti–6Al–4V substrates were obtained by a simple sedimentation process at 980 °C in an Ar atmosphere.
2. The coating containing 20 wt.% of silver nanoparticles has an excellent biocidal activity ($\log \eta > 5$) against Gram+, Gram− bacteria, and yeast. This raises the possibility for its application on titanium-based implants, such as dental and hip implants.
3. The silver lixiviation from the coatings after the biocide tests was found to be ∼10 ppm for three studied microorganisms. This amount is below the toxic limit for human osteoblasts (∼30 ppm).

Acknowledgements

This work has been supported by ITMA (Asturias, Spain) under contract number 20102141, Spanish MICINN, MAT2009-14542-C02-01 and by the National Institutes of Health (NIH/NIDCR) under grant number 5R01 DE015633.

References

1. Boodman SG, Maloney B. Replaceable you. The Washington Post; September 17 2007.
2. Schein H. *Henry Schein enters growing dental implant category through strategic partnership with camlog*. Melville, NY: Business Wire; 2004. July 6.
3. Meier B. *Absence of warranties for implants costs health system*. New York: The New York Times; 2010. April 2.
4. Pye AD, Lockhart DEA, Dawson MP, Murray CA, Smith AJ. A review of dental implants and infection. *J Hosp Infect* 2009;**72**(2):104–10.
5. Cramton SE, Gerke C, Gotz F. In vitro methods to study staphylococcal biofilm formation. *Methods Enzymol* 2001;**336**:239–55.
6. Donlan RM, Costerton JW. Biofilms: survival mechanisms of clinically relevant microorganisms. *Clin Microbiol Rev* 2002;**15**(2):167–93.
7. Bozic KJ, Ries MD. The impact of infection after total hip arthroplasty on hospital and surgeon resource utilization. *J Bone Joint Surg Am* 2005;**87**(8):1746–51.
8. Colon G, Brian CW, Webster TJ. Increased osteoblast and decreased *Staphylococcus epidermidis* functions on nanophase ZnO and TiO_2. *J Biomed Mater Res* 2006;**8**(3):595–604.
9. Singh PK, Parsek MR, Greensberg EP, Welsh MJ. A component of innate immunity prevents bacterial biofilm development. *Nature* 2002;**17**(6888):552–5.
10. Jiranek W, Hanssen A, Greenwald AS. Antibiotic-loaded bone cement for infection prophylaxis in total joint replacement. *J Bone Joint Surg Am* 2006;**8**(11):2487–500.
11. Block JE, Stubbs HA. Reducing the risk of deep wound infection in primary joint arthroplasty with antibiotic bone cement. *Orthopedics* 2005;**8**(11):1334–45.
12. Dunbar MJ. Antibiotic bone cements: their use in routine primary total joint arthroplasty is justified. *Orthopedics* 2009;**2**(9):660.
13. Hanssen AD. Prophylactic use of antibiotic bone cement: an emerging standard-in opposition. *J Arthroplasty* 2004;**9**(4):73–7.
14. Joseph TN, Chen AL, Di Cesare PE. Use of antibiotic-impregnated cement in total joint arthroplasty. *J Am Acad Orthop Surg* 2003;**1**(1):38–47.
15. Namba RS, Chen Y, Paxton EW, Slipchenko T, Fithian DC. Outcomes of routine use of antibiotic-loaded cement in primary total knee arthroplasty. *J Arthroplasty* 2009;**24**(Suppl. 6):44–7.
16. Dueland R, Spadaro JA, Rahn BA. Silver antibacterial bone cement, comparison with gentamicin in experimental osteomyelitis. *Clin Orthop Relat Res* 1982;**69**:264–8.
17. Vik H, Andersen KJ, Julshamn K, Todnem K. Neuropathy caused by silver absorption from arthroplasty cement. *Lancet* 1985;**1**(8433), 872–872.
18. Sudmann E, Vik H, Rait M, Todnem K, Andersen KJ, Julsham K, et al. Systemic and local silver accumulation after total hip replacement using silver-impregnated bone cement. *Med Prog Technol* 1994;**20**(3–4):179–84.
19. Spadaro JA, Webster DA, Becker RO. Silver polymethyl methacrylate antibacterial bone cement. *Clin Orthop Relat Res* 1979;**143**:266–70.
20. Tomsia AP, Launey M, Lee J, Mankani M, Wegst U, Saiz E. Nanotechnology approaches to improve dental implants. *Int J Oral Maxillofac Implants* 2011;**26**(Suppl):25–44.
21. Esteban-Tejeda L, Malpartida F, Pecharroman C, Moya JS. High antibacterial and antifungal activity of silver monodispersed nanoparticles embedded in a glassy matrix. *Adv Eng Mater* 2010;**12**(7):B292–7.
22. Evans PA, Stevens R, Binner JGP. Quantitative X-ray diffraction analysis of polymorphic mixes of pure zirconia. *Br Ceram Trans* 1984;**83**:39–43.
23. Esteban-Cubillo A, Díaz C, Fernández A, Díaz LA, Pecharromán C, Torrecillas R, et al. Silver nanoparticles supported on [alpha]-, [eta]- and [delta]-alumina. *J Eur Ceram Soc* 2006;**26**(1–2):1–7.
24. Mie G. Articles on the optical characteristics of turbid tubes: especially colloidal metal solutions. *Ann der Phys* 1908;**25**(3):377–445.
25. Senoy T, Saritha KN, Jamal EMA, Al-Harthi SH, Manoj Raama V, Anantharaman MR. Size-dependent surface plasmon resonance in silver silica nanocomposites. *Nanotechnology* 2008;**7**:075710.
26. Tomsia AP, Pask JA. Chemical reactions and adherence at glass/metal interfaces: an analysis. *Dent Mater* 1986;**2**(1):10–6.
27. Saiz E, Cannon RM, Tomsia AP. High-temperature wetting and the work of adhesion in metal/oxide systems. *Ann Rev Mater Res* 2008;**38**:197–226.
28. Randall MG. *Sintering theory and practice*. John Wiley and Sons; 1996.
29. Murray JL, Bhansali JK. The Ag–Ti (silver–titanium) system. *Bull Alloy Phase Diagrams* 1983;**4**(2):178–83.
30. Van Loo FJJ, Rijnders MR, Rönka KJ, Gülpen JH, Kodentsov AA. Solid state diffusion and reactive phase formation. *Solid State Ionics* 1997;**95**(1–2):95–106.
31. Panacek A, Kolar M, Vecerova R, Prucek R, Soukupova J, Krystof V, et al. Antifungal activity of silver nanoparticles against *Candida* spp. *Biomaterials* 2009;**30**(31):6333–40.
32. Zhao L, Wang H, Huo K, Cui L, Zhang W, Ni H, et al. Antibacterial nano-structured titania coating incorporated with silver nanoparticles. *Biomaterials* 2011;**32**:5706–16.
33. Song WH, Ryu HS, Hong SH. Antibacterial properties of Ag (or Pt)-containing calcium phosphate coatings formed by micro-arc oxidation. *J Biomed Mater Res A* 2008;**88**:246–54.